Available online at www.sciencedirect.com
SCIENCE DIRECT®
Journal of Catalysis 226 (2004) 401–409
JOURNAL OF CATALYSIS
www.elsevier.com/locate/jcat

Stability and distribution of cesium in Cs-promoted silver catalysts used for butadiene epoxidation

John R. Monnier [a,*,1], Jerome L. Stavinoha Jr. [b], Robin L. Minga [a]

[a] *Research Laboratories, Eastman Chemical Company, PO Box 1972, Kingsport, TN 37662, USA*
[b] *Research and Development, Texas Operations, Eastman Chemical Company, PO Box 7444, Longview, TX 75607, USA*

Received 13 April 2004; revised 28 May 2004; accepted 2 June 2004

Available online 10 July 2004

Abstract

Highly Cs-promoted Ag catalysts, such as those used for C_4H_6 epoxidation, undergo deactivation with respect to activity and selectivity for EpB formation upon storage in air. This loss in performance during storage in air is due to moisture-induced agglomeration of the Cs salt promoter. The agglomeration of the Cs promoter is reversible; calcination in air at temperatures between 200 and 300 °C efficiently redistributes the Cs over the Ag surface. For optimal performance, the Cs promoter must be evenly distributed on the Ag surface. Surface analysis by XPS confirms that calcination of such a deactivated catalyst between 150 and 300 °C increases the surface concentrations of both Cs and Cl (when CsCl is used as the promoter salt) while the concentration of surface Ag concurrently decreases. The strong positive correlation between the Cs/Ag surface ratio and the catalytic activity and selectivity supports the conclusion that an even distribution of Cs on the Ag surface is required for optimal performance of promoted catalysts for C_4H_6 epoxidation. The basis of the Cs-promoter effect is clearly electronic in nature. The fact that optimal distribution of Cs on the Ag surface increases both selectivity to EpB and activity for C_4H_6 conversion makes it very difficult to conclude that the role of Cs is only to block surface sites that lead to combustion of EpB to CO_2 and H_2O. This conclusion is also consistent with the earlier results of Monnier who showed that successful promoters for EpB catalysts were limited to Tl^+, Cs^+, and Rb^+, but not K^+. Within this series of promoters, the only noteworthy differences were not the ionic radii, but the Pauling polarizabilities, of these cations (the largest of any ions in the Periodic Table), which support the idea of electronic effects being responsible for Cs-promoted Ag catalysts for olefin epoxidation. Loss of activity upon storage for Cs-promoted Ag catalysts used for C_2H_4 epoxidation has not been reported. Catalysts used for C_4H_6 epoxidation contain much higher levels of Cs promoters (600–1400 ppm Cs) compared to catalysts used for C_2H_4 epoxidation (200–400 ppm Cs). Results in this paper show that catalyst deactivation due to storage in air is a strong function of Cs loading; deactivation for C_4H_6 epoxidation becomes negligible below approximately 560 ppm Cs, thus explaining why such deactivation has not been reported for catalysts typically used for C_2H_4 epoxidation.

Keywords: Butadiene; Epoxidation; Epoxybutene; EpB; Cs promoter; Silver catalyst; Agglomeration; Deactivation

1. Introduction

Cesium is the preferred promoter for the silver-catalyzed epoxidation of both ethylene and butadiene [1–4]. There are, however, notable differences in the amounts of cesium required for optimal catalyst performance for the two reactions as well as differences in the explanations for the promoter effect(s) of cesium. The amounts of Cs used to optimize the performance of ethylene oxide (EO) catalysts is much lower than that required for epoxybutene (EpB) catalysts. Cesium loadings for EO catalysts typically vary between 200 and 400 ppm (wt), based on total catalyst weight [5–7], while for butadiene epoxidation, Cs requirements for similar Ag weight loading catalysts are between 600 and 1400 ppm (wt), also based on total catalyst weight [3,8,9]. Like-

* Corresponding author.
E-mail address: monnier@engr.sc.edu (J.R. Monnier).
[1] Current address: Department of Chemical Engineering, University of South Carolina, Columbia, SC 29208.

0021-9517/$ – see front matter
doi:10.1016/j.jcat.2004.06.005

wise, the role of the promoter for C_2H_4 epoxidation has been shown to be primarily limited to increasing the selectivity to EO, at the expense of overall activity for C_2H_4 conversion. Lambert and co-workers have examined both conventional Cs-promoted Ag/Al_2O_3 catalysts [10] and Cs-modified Ag(111) surfaces [2,11,12] and argued convincingly that Cs improves selectivity to EO by influencing the secondary chemistry of EO, namely, that of lowering the rate of isomerization of EO to acetaldehyde, which undergoes rapid combustion to CO_2 and H_2O. Lambert further argues that the Cs effect on selectivity is not one of site blockage of isomerization sites on Ag, but is electronic in nature. Since similar improvements in selectivity are seen for both supported Ag catalysts and Ag(111) single crystal surfaces, Cs is assumed to affect the Ag surface, rather than acid sites on the Al_2O_3 surface. As expected, because the Cs is situated on the Ag surface, the overall activity for C_2H_4 conversion also decreases as the selectivity to EO increases. Minahan and co-workers [13–16] have used scanning electron microscopy (SEM) and a variety of ultrahigh vacuum spectroscopic techniques to characterize a series of fresh and aged Ag/Al_2O_3 catalysts, both unpromoted and Cs promoted. The authors concluded that while Cs does increase selectivity to EO, relative to unpromoted catalysts, it does so by improving the dispersion and coverage of Ag on the Al_2O_3 surface; Cs acts a binder between the Al_2O_3 surface and the Ag crystallites to give a more uniform and higher coverage of the Ag component. Because there is less Al_2O_3 exposed on the Cs-modified catalysts, the extent of Al_2O_3-catalyzed isomerization of EO to acetaldehyde is also lowered, resulting in higher selectivity to EO. Thus, the role of Cs is an indirect one, since it only serves to "wet" the Al_2O_3 toward Ag deposition on the support. This explanation is obviously different from the role of Cs proposed by Lambert, where the effect of Cs is direct since it modifies the Ag surface toward the Ag-catalyzed isomerization of EO to acetaldehyde, which leads to the facile combustion to CO_2 and H_2O.

Monnier and co-workers [3,9,17] have also studied the effects of Cs loadings on Cs-promoted Ag/Al_2O_3 catalysts and found that optimal Cs loadings increase not only the selectivity to EpB but also dramatically increase the activity for C_4H_6 conversion and greatly extend catalyst life. For example, while an unpromoted Ag catalyst gave approximately 50% selectivity to EpB at a C_4H_6 conversion of 1–2%, a catalyst optimally promoted with a Cs salt, such as CsCl or $CsNO_3$, increased selectivity to 95% at a C_4H_6 conversion of 15–20%. Further, catalyst life improved from only 3–4 h for the unpromoted catalysts to several months for the Cs-promoted catalyst. Monnier and co-workers have used kinetic analysis [3], ^{18}O kinetic isotope effect studies [18], and deuterium isotope effect studies [19] and concluded that Cs promoters lower the desorption energy of EpB, or its precursor, from the Ag surface. This promoter effect is electronic in nature, and not due to site-blockage phenomena, since the promoter efficiencies follow the trend $Cs^+ > Rb^+ \gg K^+$ [20], and the size of these alkali cations are not greatly different; however, the polarizabilities of the cations follow the same order as their promoter effects, consistent with electronic effects being responsible for lowering the desorption energy of EpB, or its precursor. Because the desorption energy is lowered, the lifetime of EpB on the reactive Ag surface is decreased, which lowers the extent of consecutive oxidative degradation of EpB. Further, because of more facile desorption of EpB, the fraction of vacant Ag surface sites increases, leading to higher activity for C_4H_6 conversion. Finally, catalyst fouling by condensation reactions involving adsorbed EpB is lowered by the presence of Cs, which greatly increases catalyst life.

The reasons why much higher concentrations of Cs are needed for optimal EpB formation (3–4 times higher than for EO catalysts) are not obvious; however, the higher Cs requirements for EpB catalysts raise issues regarding the stabilities of such catalysts. All cesium salts are quite hygroscopic and prone to moisture-induced agglomeration [21,22], with agglomeration being more pronounced at higher Cs salt concentrations. Thus, unless the Cs promoter forms a water-stable, or insoluble, compound with the Ag/Al_2O_3 system, one must be concerned that moisture-induced storage problems of EpB catalysts might become an issue with these catalysts.

In this paper, we, in fact, identify the existence of moisture-induced agglomeration of Cs salt promoters on Ag/Al_2O_3 catalysts and the subsequent losses in catalyst performance. We describe methods to prevent or hinder such Cs salt agglomeration [23] and from surface analyses of such catalysts, we show that for optimal promotion, Cs is evenly distributed on the Ag surface component of the Ag/Al_2O_3 catalyst.

2. Experimental

The catalysts prepared in this study used general methods that have been previously described by Neilsen [23], Neilsen and LaRochelle [24], and Monnier [25]. The catalyst support was 0.25 inch diameter, fused α-Al_2O_3 rings (wall thickness = 0.125 inch), type SA-5562 supplied by Saint-Gobain NorPro (formerly Norton) Corporation. The surface area of this support was 0.7 m^2/g with a total pore volume of 0.55 cm^3/g, and a median pore diameter of 7 μm. The Ag salt used in all preparations was silver oxalate that was dissolved in an aqueous solution of ethylenediamine. The cesium-promoter salt used for all catalysts was CsCl, which was slowly added to the stirred solution containing the dissolved silver oxalate. The amounts of CsCl added were always below the solubility limits of AgCl in aqueous amine solutions [26]. Thus, the solution contacting the Al_2O_3 rings during the impregnation step was homogeneous in both Ag and Cs salts, ensuring even distribution of all components on the Al_2O_3 support. Following tumble drying in vacuo at 60 °C, the catalyst precursors were placed in a tubular reactor and were heated in air at GHSV = 400 h^{-1}

over the temperature range 30–270 °C at a heating rate of 3 °C/min, where they underwent reductive decomposition to form promoted, metallic Ag catalysts. The samples were held at 270 °C for 2 h before being cooled in flowing air to ambient temperatures.

Cesium and Ag weight loadings were determined using atomic absorption-inductively coupled plasma (AA-ICP). Unless otherwise stated, Ag weight loadings were maintained at 13–14%. Surface analysis was determined by X-ray photoelectron spectroscopy (XPS) with a Physical Electronics (PHI) Model 5400 XPS spectrometer using monochromated Al$K\alpha$ X-rays. The analysis spot size was approximately 800 μm in diameter at a pass energy of 32 eV; analysis was conducted at a base pressure of 10^{-9} Torr. Partial catalyst ring samples (sample rings cross-sectionally split in half to expose the 0.125 inch wall thickness) were mounted in a 5 mm diameter cup on a tungsten sample holder. All analyses, both XPS and SEM, were conducted on the middle portion of the exposed wall of the ring, where previous electron microscopic analysis showed the Ag crystallite density and distribution to be the most representative of any part of the ring. Analysis of the exterior wall of the ring was often nonrepresentative, due to surface abrasion and attrition during the tumble drying step. In some of the studies, catalyst samples were pretreated at 1 atm pressure in an attached PHI 4-800 microreactor attached to the XPS spectrometer. The separate, turbo-pumped reactor was isolated from the analysis chamber by a 2.75 inch gate valve, which permitted linear transport between the pretreatment chamber and the analysis chamber. Once inside the analysis chamber, the pretreated catalyst sample was mounted on the sample stage and positioned with an attached video camera so that the center of the analysis spot was always at the same position on the catalyst surface. Thus, the same sample spot could be examined after each different pretreatment sequence. For depth profiling experiments, a PHI 04-304 ion gun was used to bombard the catalyst surface with Ar^+ ions at an energy of 3 keV to give an approximate etch rate of 1 nm/min, although for heterogeneous surfaces, the etch rate is only approximate. However, comparisons between similar samples can be made using such heterogeneous surfaces.

Several of the catalyst samples were also examined by scanning electron microscopy using a LEO scanning electron microscope Model 982, equipped with a field emission gun to determine the Ag crystallite distribution and subsequent surface concentration of the Ag sites. Each catalyst sample was analyzed at 10 different regions, with each region being 190 μm^2 in area, for a total of 1900 μm^2 altogether. Visilog software was used to analyze all images; particles of different diameters were counted and collected according to size. In this way, the concentration of Ag surface sites was determined, assuming either spherical or hemispherical particle shapes (same answer for each geometry). From the surface site concentrations, average Ag particle diameters and Ag dispersion values were calculated. Because of the large number of Ag particles that were counted, typically more than 10,000 particles per sample, the results were assumed to be at least as good as those obtained by O_2 chemisorption. Further, the results using electron microscopy gave the actual size distribution of the Ag crystallites.

Catalyst evaluations were made using the reactor and GC analytical system described in earlier publications [18,20]. Catalyst samples were ground and sieved to give particle diameters of 0.4–0.8 mm; catalyst charges of 3.0 g were used for all evaluations. Catalyst bed temperatures during reaction were measured by means of a movable chromel/alumel thermocouple (0.020 inch o.d.) inside an axial, thin-walled stainless-steel thermowell running the full length of the reactor. Tylan FC-260 mass-flow controllers were used to regulate and maintain flows of C_4H_6, O_2, and He diluent in the various reaction protocols. Unless otherwise stated, feed compositions in all experiments were maintained at 16% C_4H_6, 16% O_2, 68% He diluent at a GHSV = 14,400 h^{-1}.

3. Results

Two hundred grams of catalyst containing 13.8% Ag and 1060 ppm Cs (added as CsCl) and supported on SA-5562 Al_2O_3 rings were prepared according to the method described above. Scanning electron microscopic analysis yielded the Ag distribution shown in Fig. 1. From the distribution data and Ag weight loading, the calculated Ag dispersion was 0.011, giving an average Ag particle diameter = 0.107 μm. Note that because the Ag surface area varies as the square of the diameter, the average calculated diameter is different than that expected from the data in Fig. 1. For 1060 ppm Cs, the monodisperse distribution of Cs on the Ag surface gives a theoretical and reasonable value of $\theta_{Cs} = 0.55$. In order to examine possible storage issues, the catalyst was evenly divided into three equal samples: one portion was stored in an amber bottle in open laboratory air, another third was stored in an amber bottle in an evacuated desiccator, and the remaining sample was stored in a

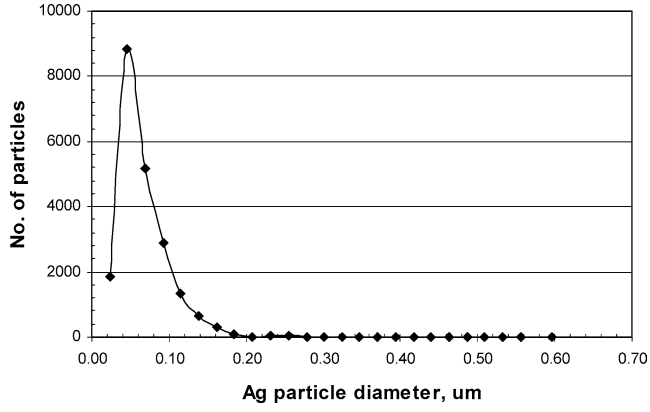

Fig. 1. Particle-size distribution of Cs-promoted Ag/Al_2O_3 catalyst containing 13.8% Ag and 1060 ppm Cs. Ag particles were well dispersed and both hemispherical and spherical in shape.

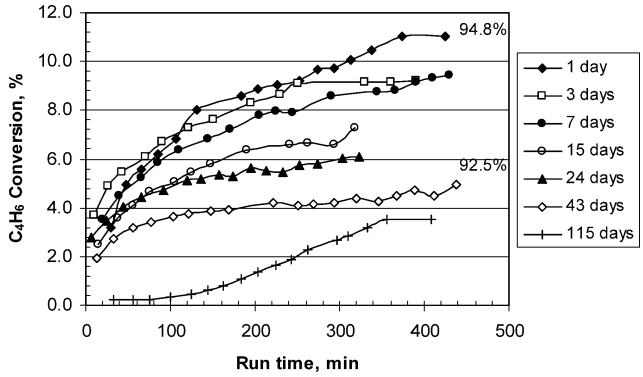

Fig. 2. Catalytic activities as a function of storage times for sample stored in amber bottle and laboratory air. Final selectivities to EpB for sample after 1 and 43 days of storage are shown adjacent to relevant run data.

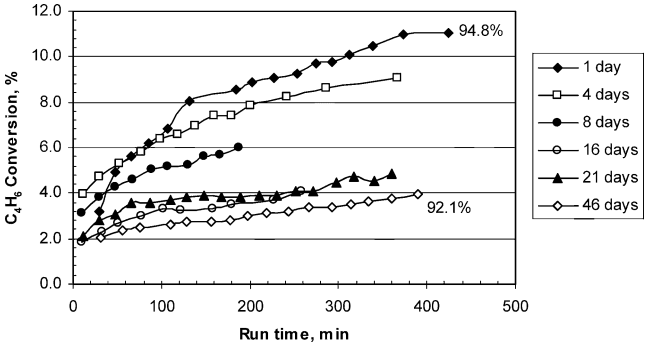

Fig. 3. Catalytic activities as a function of storage time for sample stored in clear bottle in direct sunlight. Final selectivities to EpB for samples after 1 and 46 days of storage are shown adjacent to relevant run data.

clear bottle and placed in direct sunlight. These conditions were chosen to determine whether normal ambient moisture conditions could cause Cs agglomeration and if visible light could lead to photolytically induced decomposition of the promoted catalyst, particularly if the Cl (from CsCl) existed as "AgCl" moieties and had solid-state properties typical of light-sensitive Ag halides. It is, of course, known that AgCl having extended lattice properties is light sensitive [27] in the visible spectrum.

The results in Figs. 2–4 summarize catalytic activity measurements for each of the three samples after different periods of storage. The catalyst evaluation data in Fig. 2 indicate that the sample stored in air lost over 50% of its activity as storage time increased from 1 to 43 days. Further, selectivity to EpB also declined from 94.8 to 92.5% over this time interval. Previous work [19,28] has shown that for C_4H_6 epoxidation, selectivity losses come solely from the consecutive oxidation of EpB, or its precursor. For consecutive reaction pathways, lower conversion levels of C_4H_6 to EpB should give higher, not lower, selectivities to EpB. Thus, the loss in catalyst selectivity even at lower EpB concentrations in Fig. 2 further indicated an overall decline in Cs-promoter efficiency. Earlier work using ^{18}O kinetic isotope methods [18] indicated that the desorption energy of EpB was higher with less disperse Cs loadings on Ag, which lowered both the activity and the selectivity as predicted by the kinetic and surface models described in the study. The results in Fig. 3 for the sample stored in air and direct sunlight are very similar to those results for the sample stored in air in an amber bottle, indicating that if photolysis of the CsCl-promoted Ag catalyst did occur, it did not cause loss of catalyst performance. The activity loss in Fig. 3 can be fully explained as the result of exposure to ambient laboratory air conditions. The catalyst performance data in Fig. 4 for the sample stored in a vacuum desiccator are quite different from the other samples. Catalytic activity and selectivity to EpB remained much more constant over the same 43-day storage period. Only after longer storage periods (100 days) did catalyst activity and selectivity decline to levels similar to those for the air-stored samples. These results suggest that moisture may in fact be responsible for the activity and selectivity losses observed in a more pronounced manner in Figs. 2 and 3. To better link Cs-promoter efficiency with selectivity to EpB, the data in Fig. 5 show selectivity to EpB vs C_4H_6 conversion for catalysts after 43 days of storage in air and in a vacuum desiccator. It is clear that efficient Cs promotion increases both activity and selectivity for C_4H_6 epoxidation catalysts, and that prolonged exposure to laboratory air severely degrades catalyst performance.

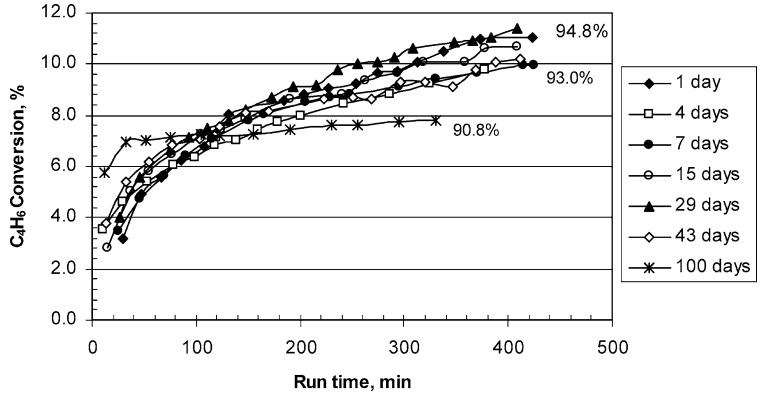

Fig. 4. Catalytic activities as a function of storage time for sample stored in amber bottle in vacuum desiccator. Final selectivities to EpB for samples after 1, 43, and 100 days of storage are shown adjacent to relevant run data.

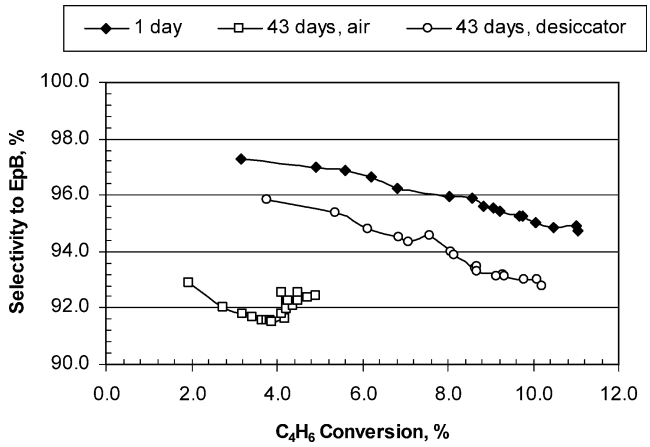

Fig. 5. Effect of storage conditions on catalyst performance for C_4H_6 epoxidation.

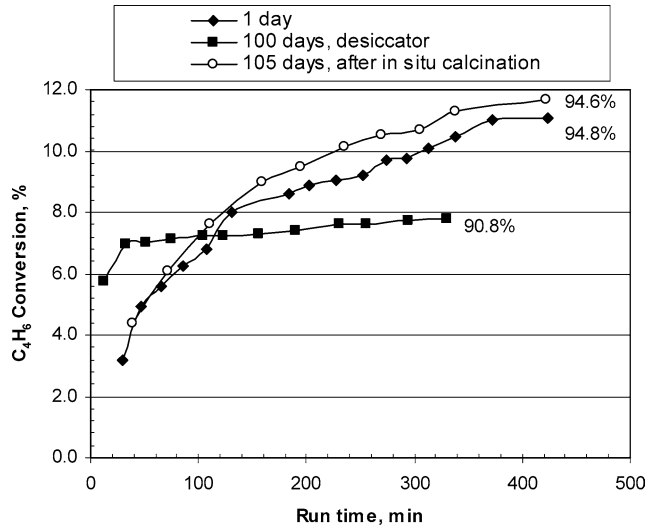

Fig. 6. Effect of in situ calcination on catalyst that had undergone activity and selectivity loss during storage. Final selectivity to EpB shown adjacent to run curve.

If moisture-related agglomeration of Cs is responsible for loss of performance, then calcination may redistribute the promoter on the catalyst surface. Results of in situ air calcination for a sample that had been stored for 105 days in a vacuum desiccator are shown in Fig. 6. Catalyst performance is essentially fully restored by calcination for 1 h at 250 °C in flowing air (GHSV = 4800 h^{-1}). In fact, air calcination has been previously used to redisperse catalysts for other types of supported catalysts. Several authors [29–31] have described in detail that air calcination of supported Ir, Pd, and Pt catalysts results in increased dispersion of the metallic components on the support surface. This redispersion is typically not observed for similar high-temperature treatments in H_2-containing gas streams, presumably because precious metal oxides (that exist during air calcination) have lower melting points and higher surface mobilities than the corresponding reduced metals; for example, the melting points of Pt and its oxides are Pt (1773 °C), PtO (550 °C), and

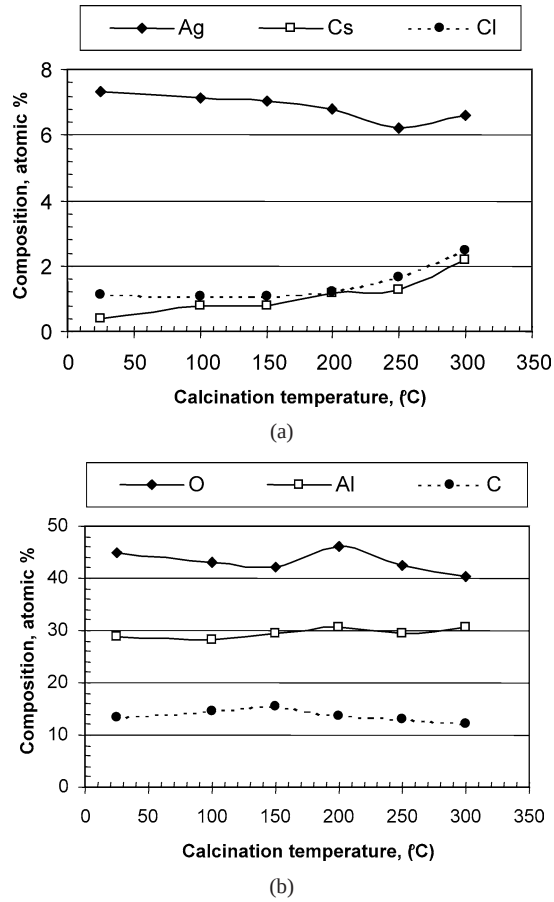

Fig. 7. (a) XPS surface analyses for Ag, Cs, and Cl concentrations after in situ calcinations at various temperatures. (b) XPS surface analyses for O, Al, and C concentrations after in situ calcination at various temperatures.

PtO_2 (450 °C). Further, metal oxides are reported to better wet support surfaces, increasing surface mobility, thus aiding in redistribution of the catalytic oxide on the support surface. While Cs oxides are clearly different from precious metal oxides, there are similarities in trends. For example, melting points of different Cs^+ oxides [32] follow the trend Cs_2O (495 °C) > CsO_2 (450 °C) > CsO_3 (70 °C). That is, the more oxygen-rich the Cs^+ oxide, the lower the melting point, presumably resulting in greater mobility of the Cs^+ oxide. Although not discussed in this paper, attempts to redistribute Cs promoters in H_2-containing gas streams were much less successful than in air calcination, in good agreement with the results of others [31].

To determine whether air calcination redispersed the Cs promoter, a series of XPS experiments were performed on a sample that had been stored in air for approximately 100 days. The sample was first analyzed “as is” and then calcined in a microreactor externally attached via a high-vacuum gate valve to the XPS spectrometer. The sample was calcined at increasingly higher temperatures for 2 h at each temperature. Since the same spot was analyzed by XPS following each calcination sequence, changes in the surface composition of the catalyst as a function of calcination temperature could be monitored. The results are summarized in Fig. 7. The

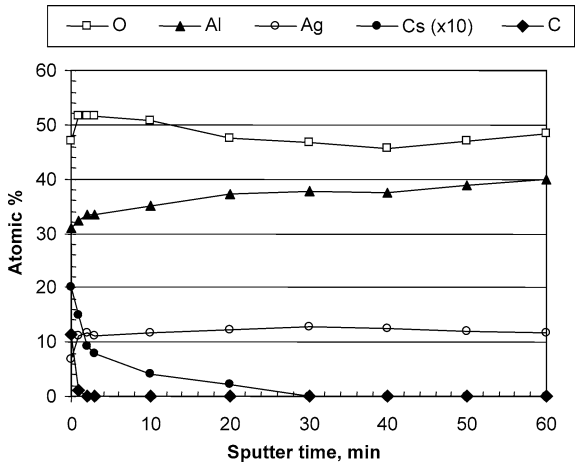

(a)

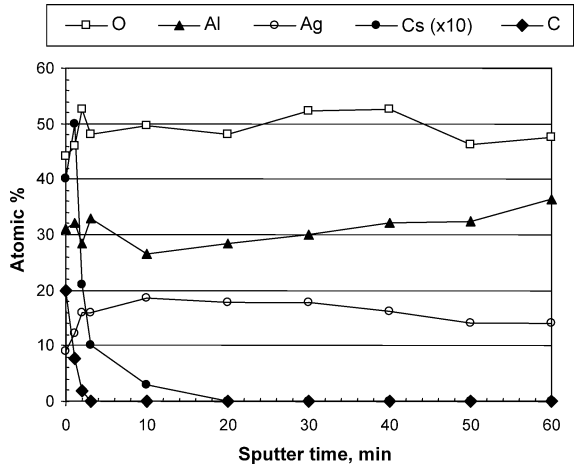

(b)

Fig. 8. (a) Sputter etch depth profile of sample stored in air for 65 days. Ar^+ at 3 keV used to etch catalyst surface. (b) Sputter etch depth profile of sample after calcination for 2 h at 250 °C followed by reaction at 225 °C for approximately 12 h.

results in Fig. 7a clearly indicate that the surface concentrations of both Cs and Cl increase as calcination temperatures increase. Since there is a concurrent decrease in surface concentration of Ag, the most reasonable explanation is that the promoter components are being redistributed on the Ag surface. The XPS data in Fig. 7b make it very difficult (order of magnitude difference in scale) to determine whether the Cs and Cl are being redistributed from the Al_2O_3 surface onto the Ag surface or whether the redistribution occurs from Cs and Cl that have agglomerated on the Ag surface, although it is much more reasonable to assume the Cs and Cl were agglomerated on the Ag surface. The sputter etch data summarized in Fig. 8 support the data of Fig. 7. The composition profile of the sample stored for 65 days (Fig. 8a) indicates that loss of Cs from the surface is accompanied by a corresponding increase in Ag concentration. Thus, as the atomic concentration of Cs decreases from 2 to 0%, the Ag surface concentration increases from approximately 8 at% to 11%. Again, no conclusions can be drawn from the Al, C, and O

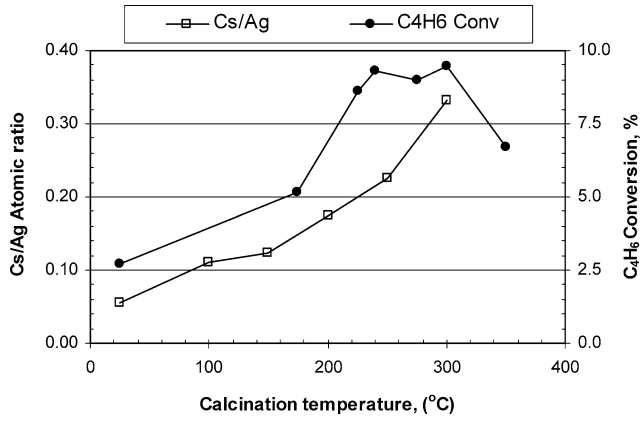

Fig. 9. Correlation of catalytic activity with the distribution of Cs on Ag.

profiles, except that the C appears to be preferentially located on the Al_2O_3 surface. Interestingly, the comparison of Figs. 8b with 8a suggests that the Cs loading for the calcined sample is more highly dispersed and evenly distributed on the Ag surface. After 10 min of sputter etching, approximately 95% of the Cs has been removed from the surface of the calcined sample, while only about 70% of the Cs has been removed after 10 min of sputter etching for the sample given no prior calcination treatment.

4. Discussion

Both catalyst evaluation data and XPS analyses indicate that the agglomeration of Cs promoters results in loss of activity and selectivity. The fact that ambient storage conditions accelerate deactivation points strongly to moisture-induced agglomeration as the cause. These results also suggest that Cs promoters can be washed from the surfaces of these catalysts. In fact, in an earlier study [33] a calcined catalyst containing 748 ppm Cs (added as CsCl) was evaluated under standard conditions to give C_4H_6 conversion of 11% and EpB selectivity of 96%; however, after washing the catalyst in water for 15 min at 50 °C, 627 ppm (or 84%) of the Cs was removed from the catalyst. Reevaluation of this catalyst gave only 1% conversion of C_4H_6 at 80% selectivity to EpB. Clearly, the Cs promoter for Cs-promoted Ag catalysts is water soluble. The correlation of the Cs distribution on Ag to catalyst performance is shown even more clearly from the data in Fig. 9, where the XPS data presented earlier are plotted as Cs/Ag vs catalyst activity (at 225 °C) for samples given the same in situ calcinations before evaluation for C_4H_6 epoxidation as the samples that were analyzed by XPS. Thus, it is possible to determine the effect of different Cs distributions on catalyst performance. There is a strong positive correlation between the Cs/Ag atomic ratio and the catalytic activity for samples calcined up to 250 °C; at temperatures above 250 °C, activity remains constant for in situ calcinations up to 300 °C. The sample calcined in situ at 350 °C is considerably less active than the samples calcined

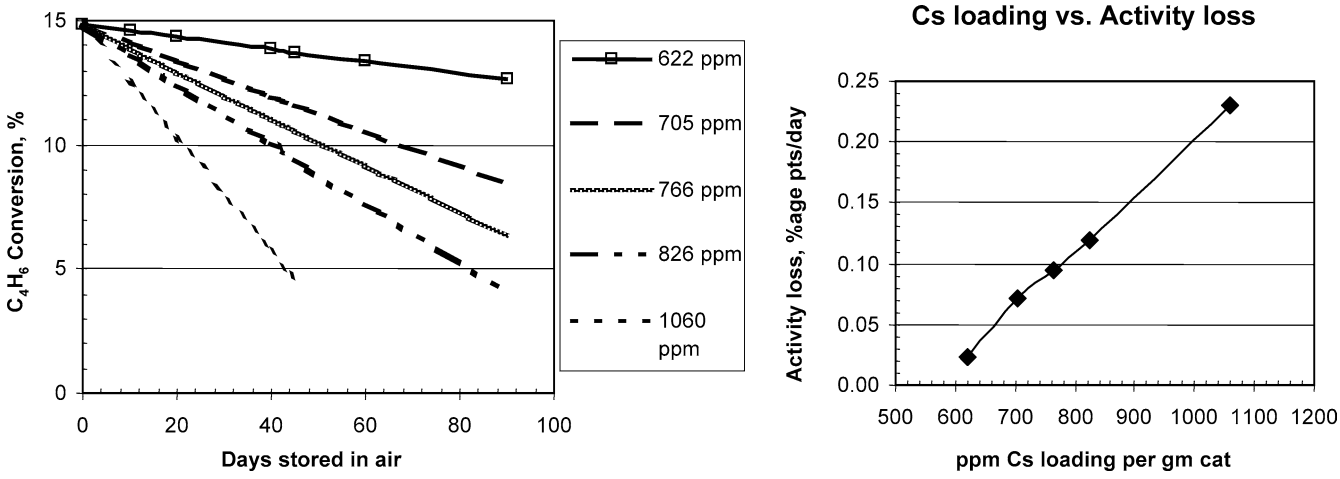

Fig. 10. Effect of Cs loading on rate of catalyst deactivation during storage in laboratory air. All catalysts prepared using same methodology and Ag loadings. Catalyst support was SA-5562 Al_2O_3 rings for all samples. (a) Least-squares fit for conversion vs storage time. Activities normalized to initial activity for sample containing 766 ppm Cs to better illustrate catalyst deactivation trends. (b) Deactivation rates in percentage points/day vs Cs loading. The fitted line intersects x axis at approximately 560 ppm Cs.

Table 1
Effect of calcination temperatures on Ag diameters

Calcination temperature (°C)	Average Ag particle diameter (μm)	Ag surface site concn. per g cat.	Ag dispersion (calc.)
None	0.107	8.47×10^{18}	0.011
150	0.105	8.63×10^{18}	0.011
250	0.109	8.32×10^{18}	0.011
300	0.121	7.46×10^{18}	0.0097
350	0.127	7.08×10^{18}	0.0092

Crystallites are assumed to have either hemispherical or spherical geometries, in good agreement with observed (by SEM) Ag particles. All calcinations conducted for 2 h in 20% O_2, 80% He.

between 220 and 300 °C. The portion of Fig. 10 showing the positive correlation between Cs/Ag and catalytic activity clearly confirms the effect of Cs distribution on Ag with catalytic activity, consistent with the strong Cs-promoter effects seen in our earlier studies [17–20]. The failure of activity to track Cs/Ag ratios at 300 °C and the fall off in activity at 350 °C is most likely due to sintering of Ag crystallites in these temperature ranges. The Tamman temperature [34] for Ag particles, the temperature at which bulk Ag atoms exhibit mobility, is approximately one-half the melting point of Ag, or 617 K, which corresponds to 344 °C. The sintering of Ag crystallites at higher calcination temperatures is confirmed by the data in Table 1, which summarizes SEM characterization data for the Cs-promoted Ag/Al_2O_3 samples after different calcination temperatures. The average Ag crystallites increase in diameter only very slightly as calcination temperatures increase to 250 °C, and a more substantial increase in size for the samples calcined at 300 and 350 °C, consistent with observations of others [34,35] for supported Ag catalysts. Since Ag surface site concentrations decrease with increasing particle size (for constant Ag weight loadings), the activity should decrease, all other factors being equal. It is also important to note that while all catalysts in this study were evaluated at 225 °C for C_4H_6 epoxidation, the catalyst evaluation temperatures did not have the same effect as the in situ calcination at temperatures as low as 200 °C. The most likely explanation is that under reaction conditions, the promoted Ag surface is almost completely covered with adsorbed C_4H_6, CO_2, and EpB, as shown earlier by Monnier and co-workers [18,19,36]. The high coverage of surface intermediates apparently restricts the redistribution of Cs on the Ag surface.

These correlations of the distribution of Cs on the Ag surface with higher activity and selectivity clearly support the conclusion that Cs directly modifies the Ag surface sites for C_4H_6 epoxidation. This interaction appears to be electronic in nature, in good agreement with the conclusions of Lambert and co-workers [10–12] for Cs-promoted Ag catalysts used for C_2H_4 epoxidation. If the role of Cs was simply to block nonselective sites on Ag or to indirectly block nonselective surface sites on the Al_2O_3 support by increasing Ag dispersion, as postulated by Minahan and co-workers [13–16], one could possibly explain the increase in selectivity to EpB as being due to site blockage, but still not account for the concurrent increase in activity for C_4H_6 conversion. The fact that both activity and selectivity increase with the optimal distribution of Cs on Ag strongly suggests that the promoter effect of Cs is electronic in origin. This is also consistent with the earlier results of Monnier and Hartley [9] who showed that while Tl^+, Cs^+, and Rb^+ showed similar promoter effects for Ag/Al_2O_3 catalysts for C_4H_6 epoxidation, K^+-promoted catalysts showed virtually no effects as a promoter. Because the ionic radius for K^+ is not appreciably smaller than those of Tl^+, Cs^+, or Rb^+, it is difficult to correlate the promoter effect present in C_4H_6 epoxidation to physical effects. As noted by Monnier and Hartley [9], the Pauling polarizabilities of Tl^+, Cs^+, and Rb^+ are the largest of any ions in the Periodic Table and much larger than that

of K^+, thus giving further support toward an electronic promoter effect for Cs-promoted Ag catalysts.

Deactivation due to storage conditions has not been reported for catalysts used for C_2H_4 epoxidation. This can be better understood by analyzing the data from an investigation of the deactivation profiles of a series of catalysts having different Cs (added as CsCl) loadings. The data in Fig. 10a show deactivation trends as a function of storage times in air for catalysts having Cs loadings ranging from 622 to 1060 ppm Cs. It is obvious that the catalysts having higher loadings of Cs deactivate at higher rates. Since deactivation due to storage in air is due to Cs agglomeration, it is intuitive that higher Cs loadings should deactivate more rapidly. In fact, the data in Fig. 10b indicate that observable deactivation using this methodology should not exist for Cs loadings less than approximately 560 ppm Cs. Since Cs loadings for EO catalysts are typically less than 400 ppm Cs, and more often in the 250–350 ppm range [4–6], it is not surprising that deactivation issues due to storage have not been discussed for these catalysts in the open literature. The reality that catalysts optimized for EpB production require more Cs and that Cs affects both activity and selectivity to EpB have permitted us to learn far more about fundamental issues and greatly increase our knowledge regarding Cs-promoted Ag catalysts used for olefin epoxidation.

5. Conclusions

Cs-promoted Ag catalysts used for C4H6 epoxidation undergo deactivation with respect to activity and selectivity for EpB formation upon storage in laboratory air. This loss in performance during storage in air is due to moisture-induced agglomeration of the Cs salt promoter. The agglomeration of the Cs is reversible; calcination in air at temperatures between 225 and 300 °C efficiently redistributes the Cs over the Ag surface. For optimal performance, the Cs promoter must be evenly distributed on the Ag surface. Surface analysis by XPS confirms that calcination of such a deactivated catalyst between 150 and 300 °C increases the surface concentrations of both Cs and Cl (when CsCl is used as the promoter salt) while the concentration of surface Ag concurrently decreases. The strong positive correlation between the Cs/Ag surface ratio and the catalytic activity and selectivity supports the conclusion that an even distribution of Cs on the Ag surface is required for optimal performance of promoted catalysts for C_4H_6 epoxidation.

The basis of the Cs-promoter effect is clearly electronic in nature, in good agreement with the results of Lambert and co-workers [10–12] for Cs-promoted Ag catalysts used for C_2H_4 epoxidation. The fact that optimal distribution of Cs on the Ag surface increases both selectivity to EpB and activity for C_4H_6 conversion makes it very difficult to conclude that the role of Cs is only to block surface sites that lead to combustion of EpB to CO_2 and H_2O. This conclusion is also consistent with the earlier results of Monnier and Hartley [9] who showed that successful promoters for EpB catalysts were limited to Tl^+, Cs^+, and Rb^+, but not K^+. Within this series of promoters, the only noteworthy differences were not the ionic radii, but the Pauling polarizabilities, of these cations (the largest of any ions in the Periodic Table), which support the idea of electronic effects being responsible for Cs-promoted Ag catalysts for olefin epoxidation.

Loss of activity upon storage for Cs-promoted Ag catalysts used for C_2H_4 epoxidation has not been reported. Catalysts used for C_4H_6 epoxidation contain much higher levels of Cs promoters (600–1400 ppm Cs) compared to catalysts used for C_2H_4 epoxidation (200–400 ppm Cs). Results in this paper show that catalyst deactivation due to storage in air is a strong function of Cs loading; deactivation for C_4H_6 epoxidation becomes negligible below approximately 560 ppm Cs, thus explaining why such deactivation has not been reported for catalysts typically used for C_2H_4 epoxidation.

Acknowledgments

As always, the authors gratefully acknowledge the efforts of Ms. Libby Cradic in helping prepare the manuscript for publication and thank Eastman Chemical Company for permission to publish this material. Finally, the efforts of Dr. Craig Sass and Mr. David Troutt in conducting the XPS and SEM analyses, respectively, are gratefully acknowledged.

References

[1] R.A. Van Santen, H.P.C.E. Kuipers, Adv. Catal. 35 (1987) 265.
[2] R.B. Grant, C.A.J. Harbach, R.M. Lambert, S.A. Tan, J. Chem. Soc., Faraday Trans. 83 (1987) 2035.
[3] J.R. Monnier, Stud. Surf. Sci. Catal. 110 (1997) 135.
[4] J.R. Monnier, P.J. Muehlbauer, US patent 4,950,773 (1990), to Eastman Kodak Company.
[5] A.M. Lauritzen, US patent 4,761,394 (1988), to Shell Oil Company.
[6] A.M. Lauritzen, US patent 4,833,261 (1989), to Shell Oil Company.
[7] B.E. Leach, in: Applied Industrial Catalysis, Academic Press, New York, 1983, pp. 207–238.
[8] J.L. Stavinoha, Jr., J.R. Monnier, D.M. Hitch, T.R. Nolen, G.L. Oltean, US patent 5,362,890 (1994), to Eastman Chemical Company.
[9] J.R. Monnier, G.W. Hartley, J. Catal. 203 (2001) 253.
[10] N. Macleod, J.M. Keel, R.M. Lambert, Catal. Lett. 86 (2003) 51.
[11] R.B. Grant, R.M. Lambert, J. Catal. 93 (1985) 92.
[12] S.A. Tan, R.B. Grant, R.M. Lambert, J. Catal. 106 (1987) 54.
[13] D.M. Minahan, G.B. Hoflund, J. Catal. 158 (1996) 109.
[14] G.B. Hoflund, D.M. Minahan, J. Catal. 162 (1996) 48.
[15] D.M. Minahan, G.B. Hoflund, W.S. Epling, D.W. Schoenfeld, J. Catal. 168 (1997) 393.
[16] W.S. Epling, G.B. Hoflund, D.M. Minahan, J. Catal. 171 (1997) 490.
[17] J.R. Monnier, P.J. Muehlbauer, US patent 4,897,498 (1990), to Eastman Kodak Company.
[18] J.R. Monnier, J.W. Medlin, M.A. Barteau, J. Catal. 203 (2001) 362.
[19] J.W. Medlin, J.R. Monnier, M.A. Barteau, J. Catal. 204 (2001) 71.
[20] J.R. Monnier, G.W. Hartley, J. Catal. 203 (2001) 253.
[21] M.C. Sneed, R.C. Brasted, in: The Alkali Metals, in: Comprehensive Inorganic Chemistry, vol. 6, Van Nostrand, Princeton, 1957, pp. 3–178.

[22] J.W. Mellor, in: Inorganic and Theoretical Chemistry, Wiley, New York, 1963, pp. 2286–2435.
[23] R.P. Neilsen, US patent 3,702,259 (1972), to Shell Oil Company.
[24] R.P. Neilsen, J.H. LaRochelle, patent 3,962,136 (1976), to Shell Oil Company.
[25] J.R. Monnier, US patent 6,455,713 (2002), to Eastman Chemical Company.
[26] W.F. Linke, in: Solubilities of Inorganic and Metal–Organic Compounds, Am. Chem. Society, Washington, DC, 1958, pp. 59–70.
[27] T.H. James (Ed.), The Theory of the Photographic Image, Eastman Kodak Company, Rochester, NY, 1977, pp. 37–50.
[28] J.R. Monnier, K.T. Peters, G.W. Hartley, J. Catal. in press.
[29] R. Gollob, D.B. Dadyburjor, J. Catal. 68 (1981) 473.
[30] E.G. Derouane, R.T.K. Baker, J.A. Dumesic, R.D. Sherwood, J. Catal. 69 (1981).
[31] J.J. Chen, E. Ruckenstein, J. Catal. 69 (1981) 254.
[32] R.H. Lamoreaux, D.L. Hildenbrand, J. Phys. Chem. Ref. Data 13 (1984) 151.
[33] J.R. Monnier, P.J. Muehlbauer, unpublished results.
[34] A.E.B. Presland, G.L. Price, D.L. Trimm, J. Catal. 26 (1972) 313.
[35] X.E. Verykios, F.P. Stein, R.W. Coughlin, J. Catal. 66 (1980) 368.
[36] M.V. Badani, J.R. Monnier, M.A. Vannice, J. Catal. 206 (2002) 29.